

# CURRENT STATUS OF DEVELOPING PEPPER-POT EMITTANCE MONITOR FOR HIGH-INTENSITY ION BEAM\*

Y. Kotaka<sup>†,1</sup>, K. Kamakura<sup>1</sup>, Y. Sakemi<sup>1</sup>, J. Ohnishi<sup>2</sup>, H. Matsuzaki<sup>3</sup>

<sup>1</sup>Center for Nuclear Study, The University of Tokyo, Wako, Japan

<sup>2</sup>Riken Nishina Center, Wako, Japan

<sup>3</sup>Micro Analysis Laboratory, Tandem accelerator, The University of Tokyo, Tokyo, Japan

## Abstract

The experiment to measure the Electric Dipole Moment (EDM) of Francium (Fr) is in progress by Center for Nuclear Study (CNS), UTokyo. Fr is produced via a nuclear fusion reaction by bombarding a gold target with  $^{18}\text{O}$  beam, requiring a beam intensity of  $18 \text{ e}\mu\text{A}$  or higher. However, the transport efficiency of the current beam line decreases to 66 % when the beam intensity exceeds  $10 \text{ e}\mu\text{A}$ . To address this issue, we are developing a pepper-pot emittance monitor (PEM) optimized for high-intensity beams. The improvements include locating the camera far from the beam line to minimize radiation damage, achieving a distance 4.1 m while maintaining the position error of 0.13 mm. Additionally, we conducted beam tests to verify measurement errors and found the results were consistent with the measurement errors estimated from the PEM structure. Furthermore, the beam shutter time 0.27 s was estimated to be acceptable up to the beam power 1000 W to prevent PEM overheating.

## INTRODUCTION

The experiment to measure Fr-EDM with the highest measurement accuracy is in progress by CNS [1]. Fr is produced by a nuclear fusion reaction by bombarding a gold target with  $^{18}\text{O}$  beam accelerated to 7 MeV/u by AVF Cyclotron. To achieve that accuracy, a beam intensity of  $18 \text{ e}\mu\text{A}$  (400 W) or higher is required. However, the beam transport efficiency is 66 % when the beam intensity exceeds  $10 \text{ e}\mu\text{A}$  [2]. To improve the beam transport efficiency, we are developing the PEM [3,4] optimized for high-intensity beams and calculate the optimized beam trajectory.

Based on the PEM developed for beams of ECR ion source (ECRIS) [5], we are developing three additional features. The first is the camera optical system locating the camera far from the beam line to minimize radiation damage. The second is the improvement of measurement error. Since the emittance of AVF cyclotron beam is typically  $20\pi \text{ mm}\cdot\text{mrad}$ , about one-tenth emittance of ECRIS beams, an angular measurement error of 0.3 mrad or less is required to calculate the beam trajectory [2]. To verify the measurement errors, beam tests were conducted at the Micro Analysis Laboratory, Tandem accelerator, UTokyo (MALT) [6]. The third is a beam shutter mechanism aimed at short-time measurements to prevent PEM overheating due to beam irradiation, and the time reached 0.27 s [2].

\* This work was supported by JSPS KAKENHI Grant Number JP20K12481.

† kotaka@cns.s.u-tokyo.ac.jp

## ESTIMATING MEASUREMENT ERROR

The measurement errors estimated from the PEM structure are described. To obtain emittances, the beam positions and angles are measured. Our PEM is shown in Fig. 1. The mask is 1 mm thick copper plate having holes whose diameter is 0.3 mm set at 2 mm interval. The image of beam passing through each hole and glowing on the fluorescent plate tilted 45 degrees is taken with digital camera through the window. The true beam position  $r_m$  constituting an emittance is any position within a mask hole, and the true beam angles  $r'_t$  are calculated by Eq. (1) and shown in the left view of Fig. 2.

$$r'_t = (r_f - r_m) / (z_f - z_m) \quad (r = x \text{ or } y) \quad (1)$$

$$r'_e = (r_f + r_e - r_c) / (z_f - z_m) \quad (r = x \text{ or } y) \quad (2)$$

where  $z$  is beam axis. The beam position ( $x, y$ ) are horizontal and vertical axes perpendicular to  $z$ -axis, respectively. The scripts  $m$  and  $f$  mean the true beam positions on the mask and fluorescent plate, respectively.

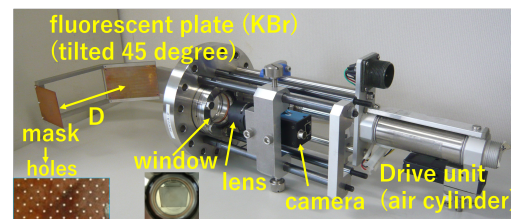


Figure 1: The developed PEM and the constituting pieces. Though this camera is close to the window in this photo, it is located far from the window to minimize radiation damage.

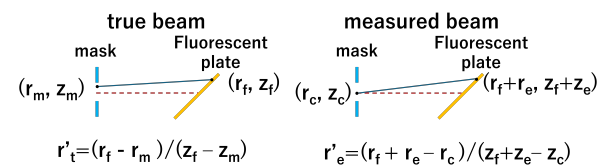


Figure 2: Definition of beam angle and the error of PEM.

However, since we know only center position  $r_c$  of the hole instead of  $r_m$ , the position error of the mask occurs in proportion to the hole radius. For the fluorescent plate, the displacement  $r_e$  from the true position  $r_f$  is added to  $r_f$

shown in the right view of Fig. 2. Since we consider these only two kind of measurement errors estimated from the PEM structure, the measured angle is defined as Eq. (2) in which we ignore the errors of  $z_c$ ,  $z_f$ , and  $z_e$  because we set the distance  $z_f - z_m$  longer than those errors.

For the position error of mask, since the hole diameter is much smaller than the beam size, we assume the beam distribution passing through a hole is uniform and regard the standard deviation (SD) of the uniform distribution as the error caused for  $r_c$ . For the diameter = 0.3 mm, the SD is 0.1 mm.

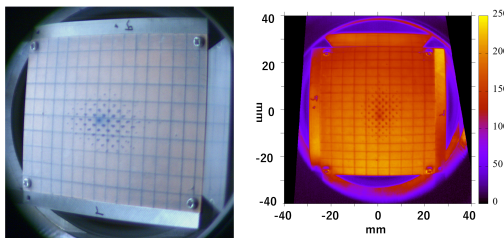


Figure 3: The left view is the fluorescent plate taken using camera with tele lens located 4.1 m away. The right view is the transformed image by the projective transformation.

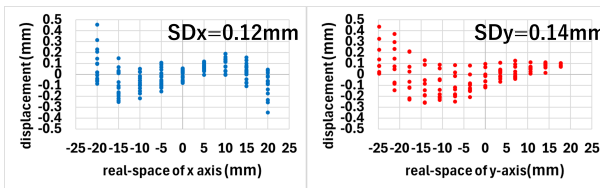


Figure 4: The relationship between the displacement of transformed positions with respect to the real space.

The position error of the fluorescent plate is described. The left view of Fig. 3 is the photo of fluorescent plate taken using a camera located 4.1 m away by combining a tele lens of the focal length 300 mm with a plane-convex lens of the focal length 200 mm to expand the camera view.

The left view of Fig. 3 on the bitmap coordinate is transformed to the right view of Fig. 3 on the real space using the projective transformation coefficients obtained by measuring the cross-point positions on the lines. The displacement of the transformed cross-point positions with respect to the correspondent real space cross-point positions are shown in Fig. 4. Since the SD of the displacements was 0.12 and 0.14 mm in  $x$  and  $y$  axes, respectively, we regard 0.13 mm on average as the position error of the fluorescent plate.

## VERIFYING MEASUREMENT ERRORS

### *The Beam Test Conducted at MALT*

We thought the measurement errors were able to estimate from the PEM structure. However, our PEM might have unknown measurement errors. To verify unknown measurement errors, we conducted beam tests at MALT, using

$^{12}\text{C}^{4+}$  beam of energy 24 MeV and intensity 1  $e\mu\text{A}$ . To verify measurement errors of PEM, we need another measured error-free emittance as a criterion. The  $\sigma$  matrixes ( $\sigma_{ij}$ ) having variances or covariances of the beam distribution in position-angle space [7] can be obtained by measuring three beam distributions [2]. The beam line has two beam profile monitors (BPM) which are BPM80 produced by National Electrostatics Corp. [8] whose error is around 0.2 mm. PEM is used as BPM with the position error of 0.1 mm.

Figure 5 shows the location of two BPMs and PEM. Two BPMs are called BPM1 and BPM2 from upstream of the beam. The distance (D) between the mask and the center of fluorescent plate shown in Fig. 1 are 269.6 mm.

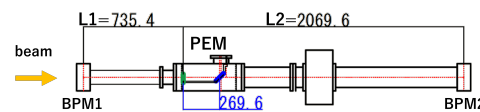


Figure 5: The location of BPM1, PEM, and BPM2. The D from mask (green) to fluorescent plate (blue) is 269.6 mm.

## *The Experimental Result and Analysis*

The beam image on the fluorescent plate obtained by beam test is shown in the Fig. 6. This image was taken using the camera placed 2.5 m away with tele lens of the focal length 100 mm. These position errors of the fluorescent plate are same as errors of Fig. 3. The beam distribution of BPM1, PEM, and BPM2 are shown in Fig. 7.

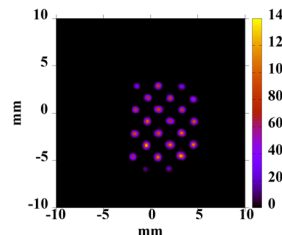


Figure 6: The beam image on the fluorescent plate.

The  $(\text{SD}_x, \text{SD}_y)$  (mm), the standard deviations of the beam distributions on  $x$  and  $y$  axes, of BPM1, PEM, and BPM2 are  $(2.8, 3.3)$ ,  $(2.3, 2.7)$ , and  $(0.3, 0.5)$ , respectively. However,  $\sigma$  matrixes were not solved because the beam distributions were neither symmetrical nor normal. By subtracting  $(0.2, 0.2)$  from  $(\text{SD}_x, \text{SD}_y)$  of PEM to get  $(2.1, 2.5)$ , a solution was obtained. The  $\sigma_{11}(\text{mm}^2)$ ,  $\sigma_{21}(\text{mm}\cdot\text{mrad})$ ,  $\sigma_{22}(\text{mrad}^2)$ ,  $\sigma_{33}(\text{mm}^2)$ ,  $\sigma_{43}(\text{mm}\cdot\text{mrad})$  and  $\sigma_{44}(\text{mrad}^2)$  at the PEM were 4.4, -1.9, 0.8, 6.5, -2.6, and 1.0, respectively. Since no coupling between  $x$  and  $y$  was observed, the other  $\sigma$  matrix elements were 0.

To search the specific error matching the PEM measurement, we used an error-free particle obtained by generating four variable normal random numbers whose SDs were the  $\sigma$  matrix elements at the PEM calculated from three BPMs.

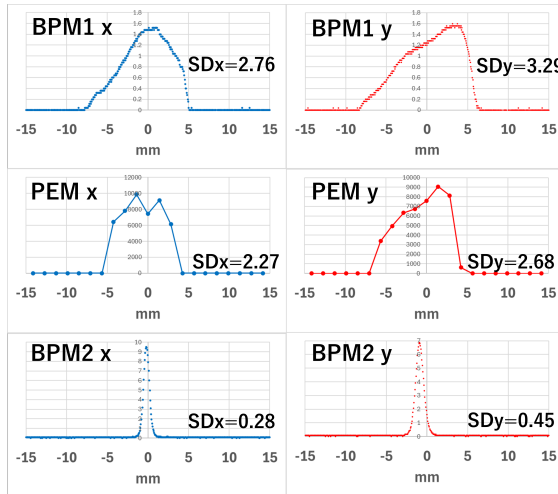


Figure 7: The beam distribution of BPM1, PEM, and BPM2 as D is 269.6 mm.

This particle corresponds to the true beam ( $x_m, x'_t, y_m, y'_t$ ) shown in the left view of Fig. 2. Next, we generated  $r_e$  as single variable normal random numbers whose SD was the position error of the fluorescent plate and added  $r_e$  to  $r_f$  shown in the right view of Fig. 2. Moreover, we displaced  $r_m$  to  $r_c$  and recalculated angles by Eq. (2). Lastly, generating  $10^6$  particles in the same way, we calculated emittances with the position errors of the fluorescent plate as variables.

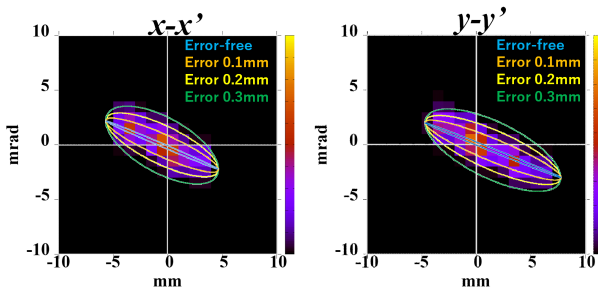


Figure 8: The comparison between the PEM measurement (contour) and the 95 % emittance calculated from the beam particles with errors (ellipses). The left and right views show the  $x-x'$  and  $y-y'$  emittances, respectively. The blue ellipse is error-free. The orange, yellow, and green ellipses are calculated by introducing the fluorescent plate position error 0.1, 0.2, and 0.3 mm, respectively.

Figure 8 shows the emittance measured by the PEM as a contour, and the 95 % emittance calculated from the beam particles with errors as an ellipse. However, the blue ellipse is error-free. The ellipses with the errors 0.1, 0.2, and 0.3 mm of the fluorescent plate are shown in orange, yellow, and green, respectively. It is found the emittance measured by the PEM matches the ellipses with the position error of the fluorescent plate between 0.1 and 0.2 mm for both  $x-x'$  and  $y-y'$ . Comparing with the position error 0.13 mm of the fluorescent plate shown in Fig. 4, Both results are consistent.

For the position error of mask, we checked the beam distributions of the error-free particles passing through the hole to verify our assumption, and found them the bell-shaped distributions whose SD was 0.08 mm for the hole diameter 0.3 mm. Though the beam distribution was not uniform, the assumed error 0.1 mm for the diameter 0.3 mm was close to 0.08 mm. Therefore, the position error of mask can be regarded as the SD of uniform distribution.

From these results, we can design a PEM with the required precision by considering only the errors from the PEM structure. For the current PEM structure, the position error of hole is 0.1 mm and the angular error are 0.6 mrad.

To achieve the required angular precision 0.3 mrad, D is estimated to be 550 mm. Besides this, we have two ideas. The first is decreasing the hole diameter of mask to 0.1 mm by etching method. The second is aiming the position error of the fluorescent plate to 0.07 mm achieved by PEM for ECRIS [5] by improving camera optical system. If they are realized, D is estimated as 252 mm.

## BEAM SHUTTER TIME

To evaluate the required beam shutter time  $t$  (s), we simulated the temperature changes  $\Delta T$  (K) of the mask made of copper using OPERA-3D when the circle area of radius 10 mm on the mask was irradiated with 1000 W beam. The thickness and area of mask were 1 mm and  $50 \times 60$  mm<sup>2</sup>, respectively. The density, specific heat, and heat conductivity of copper are  $8960$  kg/m<sup>3</sup>,  $385$  J/kgK, and  $400$  W/mK, respectively. Figure 9 shows  $\Delta T$  is around 200 K for our achieved  $t = 0.27$  and the mask is not expected to melt as  $\Delta T$  is less than copper melting point  $1084.5$  °C.

For the mask hole diameter 0.1 mm to shorten D, etching method requires 0.1 mm thickness. When the 0.1 mm thick copper is irradiated with 1000 W beam,  $\Delta T$  is calculated to be 900 K in 0.1 s. This problem should be considerable.

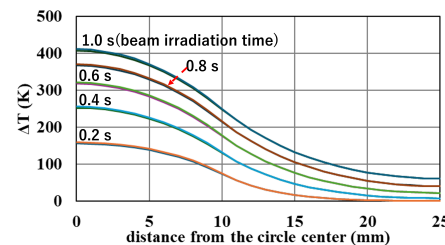


Figure 9: The distribution on the radial axis of temperature changes with respect to beam irradiation time.

## CONCLUSION

The distance between the camera and PEM reached 4.1 m by using a tele lens of the focal length 300 mm. By the beam test at MALT, we were able to verify the measurement errors of PEM can be estimated from the PEM structure. Therefore, it became possible to design any PEM with the required measurement precision. The beam shutter time of 0.27 s was estimated to be acceptable to prevent PEM overheating against beam power 1000 W.

## REFERENCES

- [1] Y. Sakemi *et al.*, “Fundamental physics with cold radioactive atoms”, *AIP Conf. Proc.*, vol. 2319, no. 1, pp. 080020, 2021.  
doi:10.1063/5.0037134
- [2] Y. Kotaka *et al.*, “Development of pepper-pot emittance monitor for High-Intensity ion beam accelerated by RIKEN AVF Cyclotron”, in *Proc. IBIC'23*, Saskatoon, Canada, Sep. 2023, pp. 339–342. doi:10.18429/JACoW-IBIC2023-WEP006
- [3] T. Hoffmann *et al.*, “Emittance measurements of high current heavy ion beams using a single shot pepperpot system”, *AIP Conf. Proc.*, vol. 546, pp. 432–439, 2000.  
doi:10.1063/1.1342615
- [4] L. E. Collins and P. T. Stroud, “Extraction of high current ion beams with low divergence”, *Nucl. Instrum. Methods*, vol. 26, pp. 157-166, 1964.  
doi:10.1016/0029-554X(64)90067-9
- [5] Y. Kotaka *et al.*, “Development of the Calculation Method of Injection Beam Trajectory of RIKEN AVF Cyclotron with 4D Emittance Measured by the Developed Pepper-Pot Emittance Monitor”, in *Proc. IBIC'19*, Malmö, Sweden, Sep. 2019, pp. 351–354. doi:10.18429/JACoW-IBIC2019-TUPP022
- [6] Micro Analysis Laboratory, Tandem accelerator website, The University of Tokyo, <https://malt.um.u-tokyo.ac.jp/>
- [7] D. C. Carey, K. L. Brown and F. Rothacker, “Third-Order TRANSPORT with MAD Input A Computer Program for Designing Charged Particle Beam Transport Systems”, Rep. FERMILAB-Pub-98/310, 1998.
- [8] *Instruction Manual for Operation and Service of Beam Profile Monitor Model BPM80*, National Electrostatics Corp., Middleton, WI, USA, Oct. 2019, <https://www.pelletron.com/wp-content/uploads/2017/02/BPM-v3.pdf>